

## Supplementary information

### A thiocarbonyl-containing small molecule for optoelectronics

David Gendron<sup>a</sup>, Fatemeh Maasoumi<sup>a</sup>, Ardalan Armin<sup>a</sup>, Katherine Pattison<sup>b</sup>, Paul L. Burn<sup>a\*</sup>, Paul Meredith<sup>b\*</sup>, Ebinazar B. Namdas<sup>b</sup>, Benjamin J. Powell<sup>b</sup>

<sup>a</sup>Centre for Organic Photonics & Electronics, School of Chemistry and Molecular Biosciences, The University of Queensland, St Lucia, QLD 4072, Australia.

<sup>b</sup>Centre for Organic Photonics & Electronics, School of Mathematics and Physics, The University of Queensland, St Lucia, QLD 4072, Australia

\*E-mail: p.burn2@uq.edu.au, meredith@physics.uq.edu.au

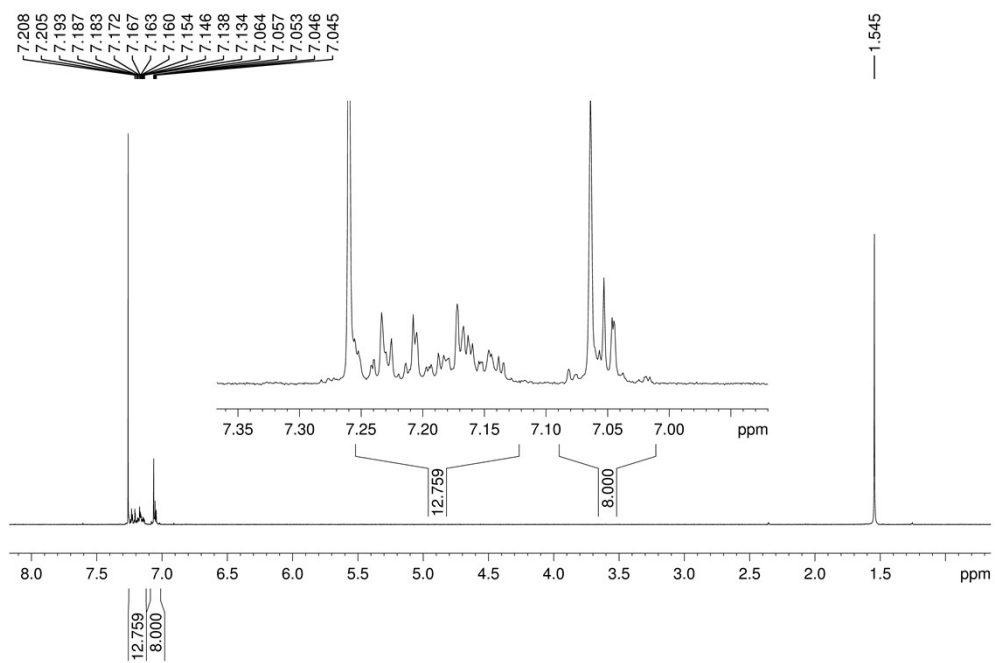


**Figure S1.**  $^1\text{H}$  NMR spectra of compound **2** at 300 K in  $\text{CDCl}_3$  ( $\delta = 7.26$  ppm).

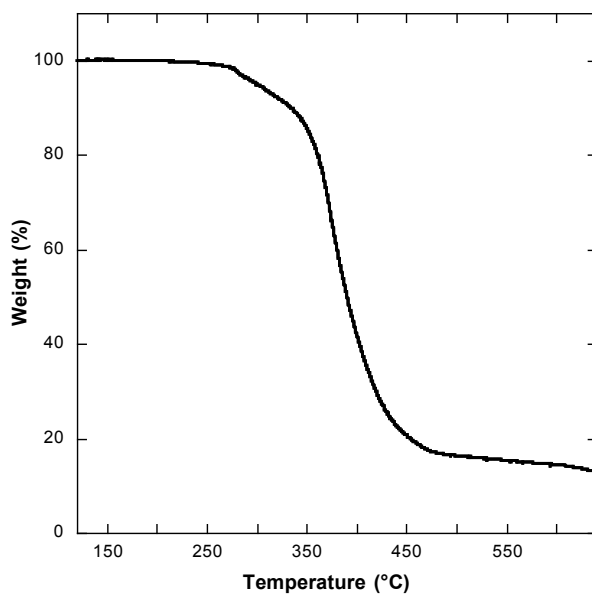


**Figure S2.** Thermogravimetric analysis of compound **2** (scan rate =  $10^{\circ}\text{C}/\text{min}$ ).

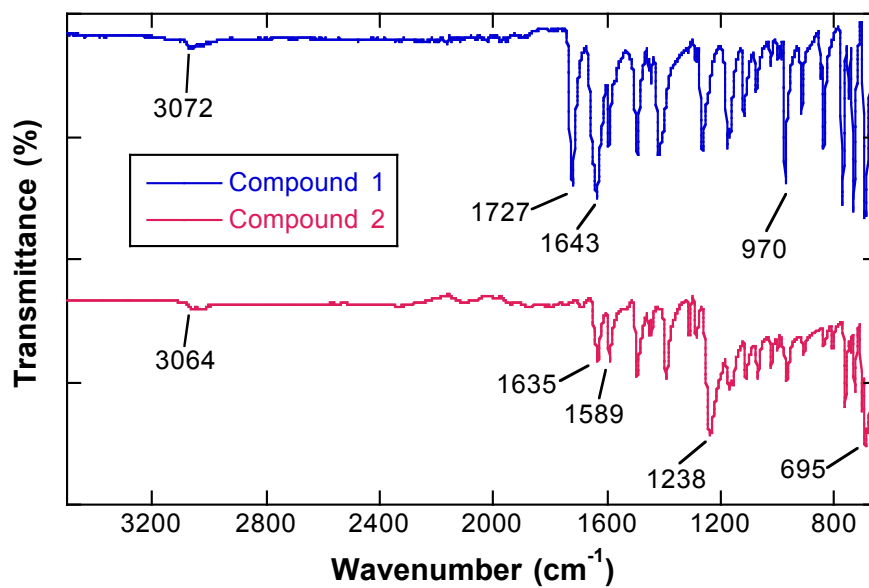


**Figure S3.** FTIR spectra of compounds **1** and **2**.

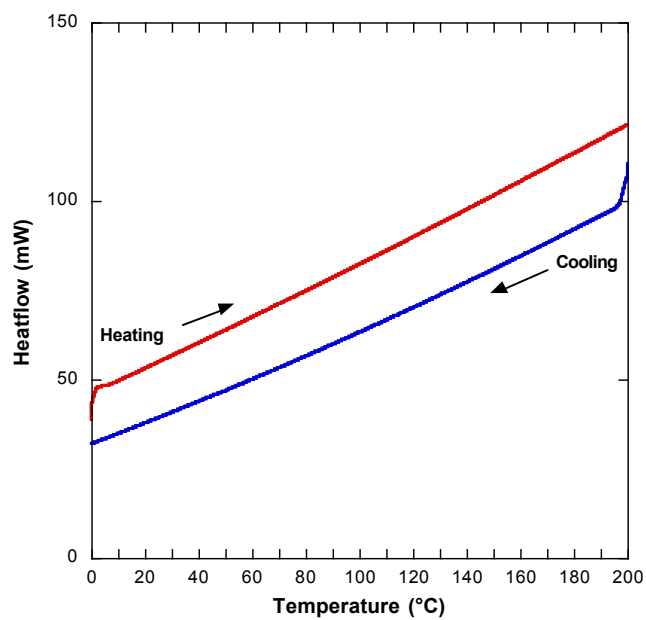


**Figure S4.** Differential scanning calorimetry of compound **2** (scan rate = 50  $^{\circ}\text{C}/\text{min}$ ).

## Detailed DFT results for compound 2

Equivalent information for compound 1 was reported in the supplementary information of our previous publication.<sup>1</sup>

### Geometry optimization

We were unable to crystallize 2 therefore we optimized the geometry using the GAMESS suite of programs.<sup>2,3</sup> This calculation was performed at the B3LYP/6-31G enforcing C<sub>i</sub> symmetry. The initial geometry was based on the measured crystal structure of 1. The resultant geometry is reported in Table S1.

**Table S1.** Calculated structure of compound 2.

| Nuclear charge (Z) | x [Å]        | y [Å]        | z [Å]        |
|--------------------|--------------|--------------|--------------|
| 6                  | -0.06154798  | -2.090677568 | 0.544943503  |
| 6                  | 0.06154798   | 2.090677568  | -0.544943503 |
| 6                  | -1.171650593 | 1.296128687  | -0.252428911 |
| 6                  | 1.171650593  | -1.296128687 | 0.252428911  |
| 6                  | -0.730100668 | 0.030509561  | 0.023576956  |
| 6                  | 0.730100668  | -0.030509561 | -0.023576956 |
| 6                  | -2.499196956 | 1.905548162  | -0.191404932 |
| 6                  | 2.499196956  | -1.905548162 | 0.191404932  |
| 6                  | -2.836551224 | 3.009480713  | -0.99968238  |
| 6                  | 2.836551224  | -3.009480713 | 0.99968238   |
| 6                  | -4.091846567 | 3.605946476  | -0.895634279 |
| 6                  | 4.091846567  | -3.605946476 | 0.895634279  |
| 6                  | -5.033089391 | 3.123231853  | 0.017989425  |
| 6                  | 5.033089391  | -3.123231853 | -0.017989425 |
| 6                  | -4.707765219 | 2.034942803  | 0.832053321  |
| 6                  | 4.707765219  | -2.034942803 | -0.832053321 |
| 6                  | -3.456242482 | 1.432988767  | 0.729435309  |
| 6                  | 3.456242482  | -1.432988767 | -0.729435309 |

|    |              |              |              |
|----|--------------|--------------|--------------|
| 6  | -2.517250428 | -1.731367801 | 0.121215547  |
| 6  | 2.517250428  | 1.731367801  | -0.121215547 |
| 6  | -3.075823628 | -2.648635065 | 1.018812574  |
| 6  | 3.075823628  | 2.648635065  | -1.018812574 |
| 6  | -4.338603702 | -3.183220113 | 0.758899829  |
| 6  | 4.338603702  | 3.183220113  | -0.758899829 |
| 6  | -5.051991278 | -2.799340774 | -0.37959148  |
| 6  | 5.051991278  | 2.799340774  | 0.37959148   |
| 6  | -4.491775951 | -1.877756708 | -1.267301788 |
| 6  | 4.491775951  | 1.877756708  | 1.267301788  |
| 6  | -3.224112964 | -1.349383593 | -1.025727378 |
| 6  | 3.224112964  | 1.349383593  | 1.025727378  |
| 7  | -1.208640441 | -1.217567312 | 0.354350446  |
| 7  | 1.208640441  | 1.217567312  | -0.354350446 |
| 16 | -0.15936604  | -3.255530161 | 0.873940408  |
| 16 | 0.15936604   | 3.255530161  | -0.873940408 |
| 1  | -2.159748157 | 3.372448757  | -1.755380566 |
| 1  | 2.159748157  | -3.372448757 | 1.755380566  |
| 1  | -4.341685401 | 4.443744504  | -1.53987482  |
| 1  | 4.341685401  | -4.443744504 | 1.53987482   |
| 1  | -6.009552595 | 3.591556636  | 0.096156152  |
| 1  | 6.009552595  | -3.591556636 | -0.096156152 |
| 1  | -5.430280741 | 1.653496699  | 1.547225103  |
| 1  | 5.430280741  | -1.653496699 | -1.547225103 |
| 1  | -3.203662427 | 0.603213619  | 1.379170275  |
| 1  | 3.203662427  | -0.603213619 | -1.379170275 |
| 1  | -2.570015045 | -2.899365455 | 1.938927704  |
| 1  | 2.570015045  | 2.899365455  | -1.938927704 |
| 1  | -4.773458763 | -3.887749694 | 1.46101568   |
| 1  | 4.773458763  | 3.887749694  | -1.46101568  |

|   |              |              |              |
|---|--------------|--------------|--------------|
| 1 | -6.037558951 | -3.212283524 | -0.570630144 |
| 1 | 6.037558951  | 3.212283524  | 0.570630144  |
| 1 | -5.040715357 | -1.569732855 | -2.151678866 |
| 1 | 5.040715357  | 1.569732855  | 2.151678866  |

### Kohn-Sham molecular orbital energies

**Table S2.** Kohn-Sham molecular orbital energies.

| Molecular | Symmetry       | Orbital Energy (eV) |
|-----------|----------------|---------------------|
| HOMO-2    | A <sub>g</sub> | -5.702              |
| HOMO-1    | A <sub>u</sub> | -5.587              |
| HOMO      | A <sub>g</sub> | -5.575              |
| LUMO      | A <sub>u</sub> | -2.219              |
| LUMO+1    | A <sub>u</sub> | -0.782              |
| LUMO+2    | A <sub>g</sub> | -0.760              |

### Excitation energies form TDDFT

**Table S3.** Singlet energies calculated via TDDFT.

|                | Symmetry       | Energy (eV) | f (a.u.) | Largest molecular orbital contributions                                 |
|----------------|----------------|-------------|----------|---|
| S <sub>1</sub> | A <sub>u</sub> | 2.56781     | 2.33E-03 | HOMO-2 → LUMO (84 %),<br>HOMO → LUMO (14 %),<br>HOMO-3 → LUMO+2 (0.5%)  |
| S <sub>2</sub> | A <sub>g</sub> | 2.66531     | 0        | HOMO-1 → LUMO (97%),<br>HOMO-3 → LUMO (1 %),<br>HOMO-1 → LUMO+1 (0.4 %) |
| S <sub>3</sub> | A <sub>g</sub> | 3.12225     | 0        | HOMO-3 → LUMO (93%),<br>HOMO-2 → LUMO+2 (2%),<br>HOMO-2 → LUMO (1%)     |
| S <sub>4</sub> | A <sub>u</sub> | 3.17684     | 0.51     | HOMO → LUMO (80%),<br>HOMO-2 → LUMO (14%),<br>HOMO-4 → LUMO (3%)        |
| S <sub>5</sub> | A <sub>u</sub> | 3.79088     | 9.41E-02 | HOMO-4 → LUMO (91%),  |

|                 |                |         |          |   |
|-----------------|----------------|---------|----------|---|
|                 |                |         |          | HOMO → LUMO (3%),<br>HOMO-1 → LUMO+2 (2%)                               |
| S <sub>6</sub>  | A <sub>g</sub> | 3.9662  | 0        | HOMO-5 → LUMO (89%),<br>HOMO-2 → LUMO+2 (2%),<br>HOMO → LUMO+2 (2%)     |
| S <sub>7</sub>  | A <sub>u</sub> | 4.02971 | 1.65E-02 | HOMO-2 → LUMO+1 (48%),<br>HOMO → LUMO+1 (14%),<br>HOMO-1 → LUMO+2 (11%) |
| S <sub>8</sub>  | A <sub>g</sub> | 4.03344 | 0        | HOMO-2 → LUMO+2 (44%),<br>HOMO-1 → LUMO+1 (19%),<br>HOMO → LUMO+2 (11%) |
| S <sub>9</sub>  | A <sub>u</sub> | 4.09153 | 6.87E-03 | HOMO-6 → LUMO (84%),<br>HOMO → LUMO+1 (4%),<br>HOMO-2 → LUMO+1 (3%)     |
| S <sub>10</sub> | A <sub>g</sub> | 4.18182 | 0        | HOMO-7 → LUMO (78%),<br>HOMO-1 → LUMO+1 (12%),<br>HOMO → LUMO+3 (3%)    |

**Table S4.** Triplet energies calculated via TDDFT.

|                | Symmetry       | Energy (eV) | f (a.u.) | Largest molecular orbital contributions                                   |
|----------------|----------------|-------------|----------|---|
| T <sub>1</sub> | A <sub>u</sub> | 2.0677      | 0        | HOMO → LUMO (94 %),<br>HOMO-2 → LUMO (1 %),<br>HOMO-10 → LUMO (1 %)       |
| T <sub>2</sub> | A <sub>g</sub> | 2.27969     | 0        | HOMO-1 → LUMO (95 %),<br>HOMO-11 → LUMO (0.9 %),<br>HOMO → LUMO+4 (0.9 %) |
| T <sub>3</sub> | A <sub>u</sub> | 2.33633     | 0        | HOMO-2 → LUMO (93%),<br>HOMO → LUMO (1%),<br>HOMO-3 → LUMO+2 (1%)         |
| T <sub>4</sub> | A <sub>g</sub> | 2.84039     | 0        | HOMO-3 → LUMO (86%),<br>HOMO-2 → LUMO+2 (5%),<br>HOMO-2 → LUMO+8 (2%)     |
| T <sub>5</sub> | A <sub>u</sub> | 3.47813     | 0        | HOMO-4 → LUMO (58%),<br>HOMO → LUMO+1 (14%),<br>HOMO-10 → LUMO (3%)       |
| T <sub>6</sub> | A <sub>g</sub> | 3.57457     | 0        | HOMO-1 → LUMO+1 (24%),<br>HOMO → LUMO+4 (19%),<br>HOMO-7 → LUMO (10%)     |
| T <sub>7</sub> | A <sub>u</sub> | 3.64001     | 0        | HOMO-1 → LUMO+2 (28%),<br>HOMO-1 → LUMO+4 (13%),<br>HOMO → LUMO+1 (11%)   |
| T <sub>8</sub> | A <sub>g</sub> | 3.68453     | 0        | HOMO-1 → LUMO+1 (22%),  |

|                 |                |         |   |   |
|-----------------|----------------|---------|---|---|
|                 |                |         |   | HOMO-4 → LUMO+2 (10%),<br>HOMO-5 → LUMO (9%)                          |
| T <sub>9</sub>  | A <sub>u</sub> | 3.72971 | 0 | HOMO-4 → LUMO (29%),<br>HOMO → LUMO+1 (19%),<br>HOMO-1 → LUMO+2 (18%) |
| T <sub>10</sub> | A <sub>g</sub> | 3.81044 | 0 | HOMO-5 → LUMO (42%),<br>HOMO-2 → LUMO+2 (11%),<br>HOMO → LUMO+2 (10%) |

### OFET characterization

The top-contact bottom-gate OFET devices, as schematically shown in Fig. 3 were comprised of a 500 nm thick SiO<sub>2</sub> dielectric layer that was thermally grown on top of a heavily n-doped silicon wafer purchased from Silicon Quest, International, Inc. The SiO<sub>2</sub> substrates were cleaned in a Class 1000 clean room using ultra-sonication in acetone for 20 min followed by ultra-sonication in 2-propanol for 20 min. Substrates were then dried under nitrogen. All the remaining fabrication steps and testing were performed inside a nitrogen filled MBraun glove box (O<sub>2</sub> and H<sub>2</sub>O levels < 0.1 ppm). The dielectric layer was treated with *n*-octyltrichlorosilane (OTS), divinyltetramethyldisiloxane-bis(benzocyclobutane) (BCB), or poly(methylmethacrylate) (PMMA).

Substrates treated with OTS were soaked for 24 h in a 3 mM solution of OTS in toluene before removal, rinsing with toluene and thermal annealing at 70 °C for 10 min. Solution of BCB was purchased from Dow Chemicals, was dissolved in mesitylene and diluted to a concentration of 5%. The BCB solution was spin-coated onto substrates at 2500 rpm for 30 s and then the films were annealed at 250 °C for 1 h to promote crosslinking.<sup>4,5</sup> A PMMA (120,000 g/mol) solution of concentration 35 mg/ml in *n*-propylacetate (P99.5%) was spin-coated onto the substrates at 2500 rpm for 30 s. The substrates were then baked on a hotplate at 150 °C for 30 min. The BCB and PMMA film thicknesses were measured to be about 260 nm and 140 nm respectively using a Dektak 150 profilometer. Compound 2 films were then spin-coated from 15mg/ml solutions using neat chloroform (CF) or CF + 5% 1,2-dichlorobenzene (ODCB) at 700 rpm for 60 sec, which gave films with thicknesses about 70 nm. Gold top contacts (40nm) were vacuum deposited through shadow masks prepared by deep reactive ion etching with a channel length 80 μm and channel width 16 μm. The electrical characteristics of the devices were tested using an

Agilent B1500A semiconductor Device Analyzer and SA-6 Semi-Auto Probe Station. The field-effect mobility ( $\mu$ ) in  $\text{cm}^2/\text{V}\cdot\text{s}$  was calculated in saturation regime of the I-V curves using the MOSFET equation:

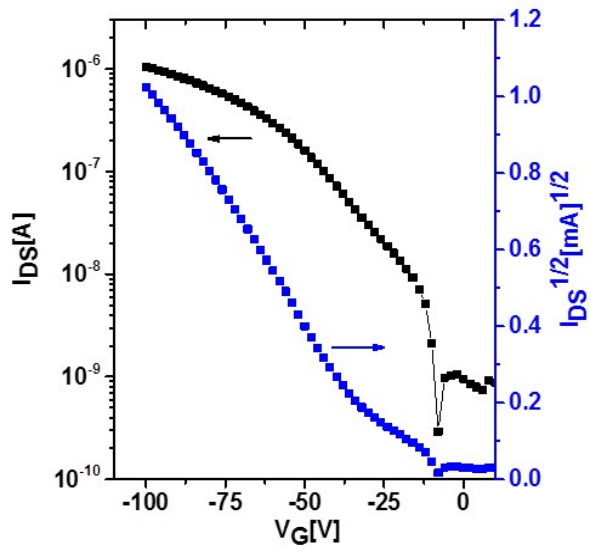
$$\mu_{sat} = \left( \frac{2L}{\omega C_i} \right) \left[ \frac{\partial \sqrt{I_{DS}}}{\partial V_g} \right]^2$$

Where  $C_i$  is the insulator capacitance,  $\omega$  and  $L$  are channel width and length, respectively,  $I_{DS}$  is the Source-Drain current and  $V_g$  is the gate voltage.

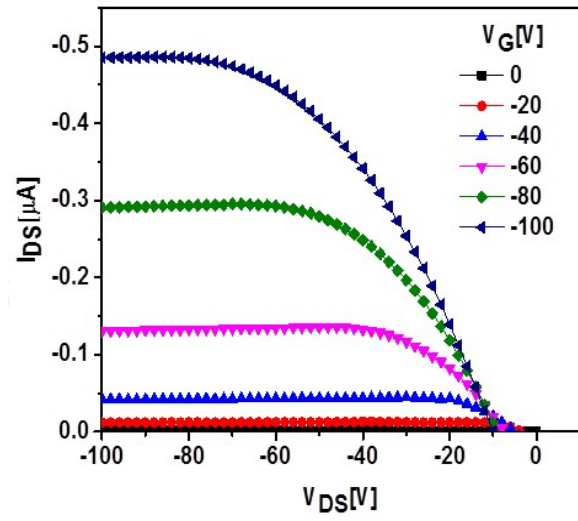
**Table S5.** Effect of the passivation layer on the FET characteristics.

| Entry | Solvent                       | Passivation layer | Hole mobility<br>$\times 10^{-4} \text{ cm}^2 \text{ V}^{-1} \text{ s}^{-1}$ | On/Off ratio<br>$\times 10^3$ | $V_{Th}$<br>V |
|-------|-------------------------------|-------------------|--|-------------------------------|---------------|
| 1     | $\text{CHCl}_3$               | OTS               | 2.2  | 3.6                           | -4            |
| 2     | $\text{CHCl}_3 + 5\%$<br>ODCB | OTS               | 1.9  | 2.2                           | -19           |
| 3     | $\text{CHCl}_3 + 5\%$<br>ODCB | BCB               | 3.1  | 3.2                           | -40           |
| 4     | $\text{CHCl}_3 + 5\%$<br>ODCB | PMMA              | 1.5  | 1.8                           | -2            |

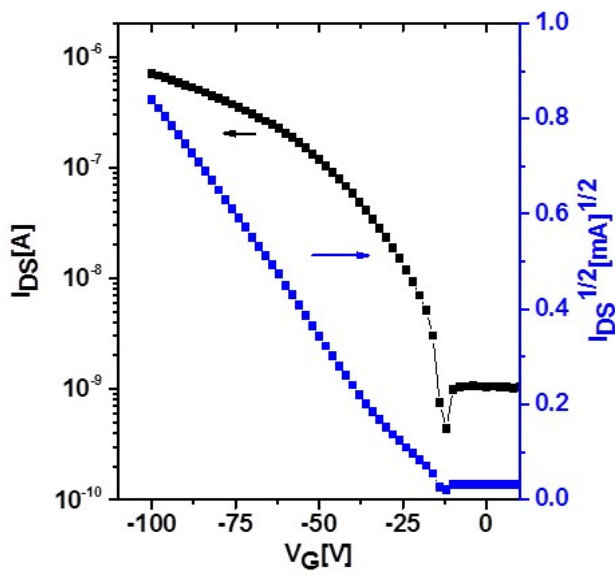
a)



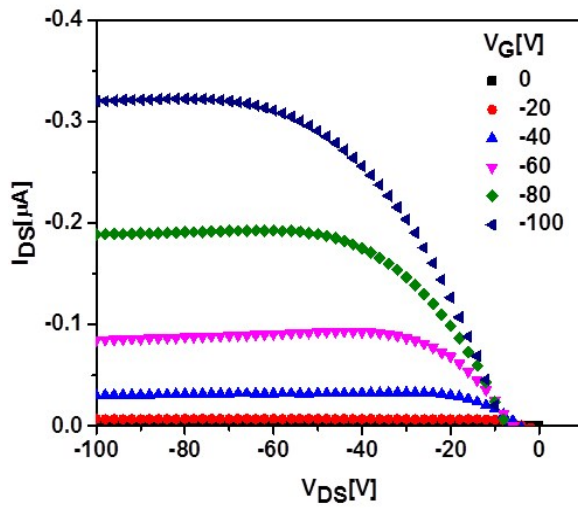
b)



c)



d)



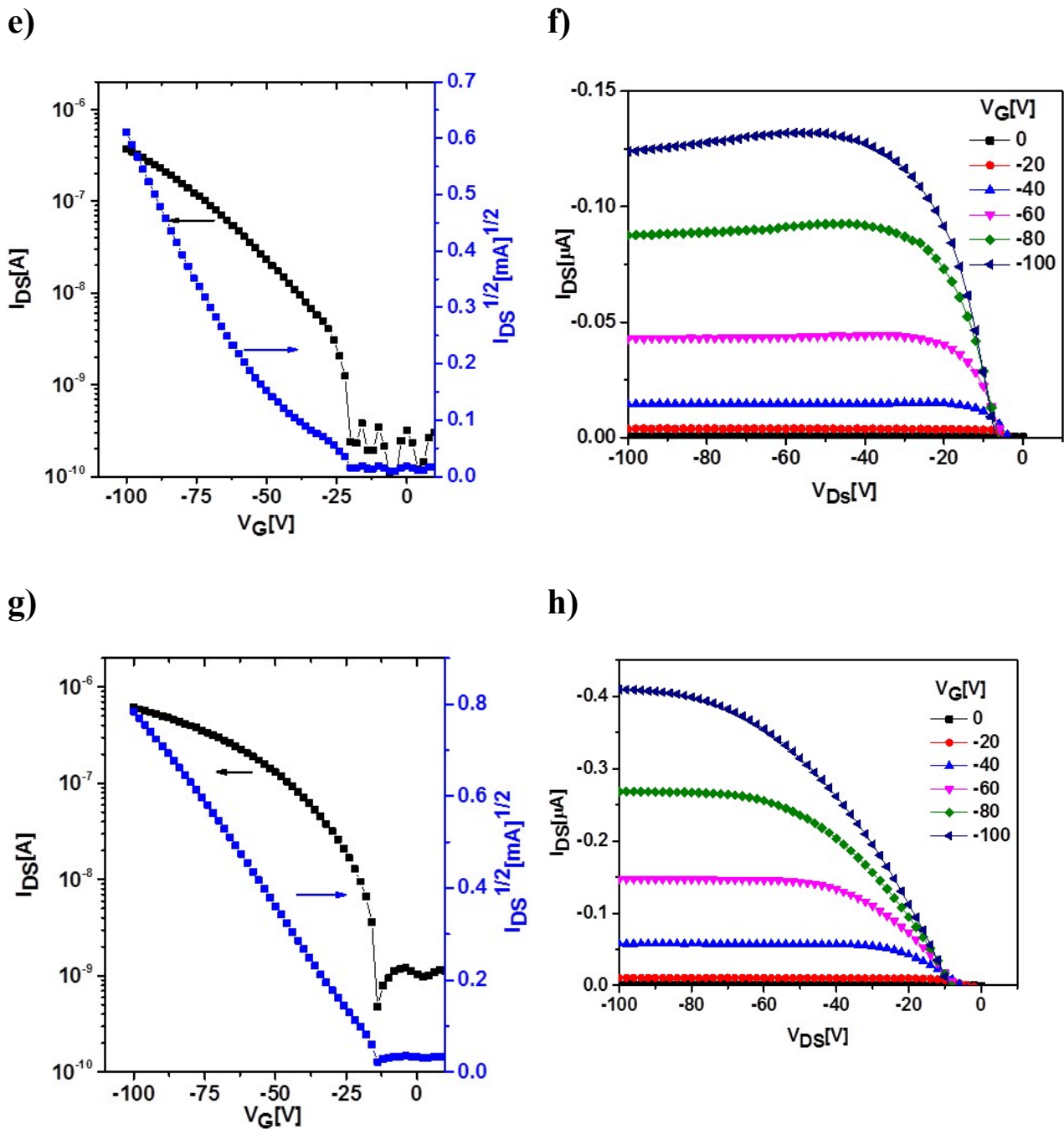


**Figure S5.** Performance of OFETs based on neat films of **2** a) Output curve of entry 1, b) Transfer curve of entry 1, c) Output curve of entry 2, d) Transfer curve of entry 2 e) Output curve of entry 3 f) Transfer curve of entry 3, g) Output curve of entry 4 h) Transfer curve of entry 4.

## OPV characterization

*Solar cell device fabrication:* pre-patterned Indium tin oxide (ITO) on glass (80 nm) substrates with sheet resistance of 15  $\Omega$ /sq. (Purchased from Kintec) were pre-cleaned using Alconox (detergent) in deionized water, and then mechanically scrubbed with a soft cloth. The ITO was then sonicated in sequence with Alconox, de-ionized water, acetone and 2-propanol for 10 min in each step. A 25 $\pm$ 5 nm layer of poly(3,4-ethylenedioxythiophene):poly(styrene sulfonate) (PEDOT:PSS) purchased from Heraeus was then spin-coated onto the ITO at 5000 rpm for 60 sec. The PEDOT:PSS layer was baked for 10 min at 170  $^{\circ}$ C in air. Solutions of 2:PC<sub>70</sub>BM at different concentrations (see below) were spin-coated at 500 r.p.m. onto the PEDOT:PSS layer in a nitrogen glovebox (O<sub>2</sub> <1 ppm, H<sub>2</sub>O <1 ppm) at  $\sim$ 20  $^{\circ}$ C. The thickness of the BHJ layer was measured by a Veeco Dektak150 profilometer. Finally, 1 nm of samarium and 80 nm of aluminium were deposited to complete the device by thermal evaporation under a 10<sup>-6</sup> mbar vacuum. The device area was 0.2 cm<sup>2</sup> with 6 devices per substrate.

*2:PC<sub>70</sub>BM deposition:* Chloroform (CF) and its mixture with 7% ODCB were used to dissolve **2** and PC<sub>70</sub>BM. Neat 100 nm thick films of **2** from CF were prepared from a solution with a concentration of 15 mg/mL. To deposit 2:PC<sub>70</sub>BM blend films from CF, a total concentration of 10 mg/mL was used and this resulted in 110 nm thick films. The wet film was monitored visually during the spin-coating process, and the rotation was stopped when the Newton rings disappeared.

*Solar cell efficiency measurement:* Light current-voltage curves were measured under simulated AM1.5G ( $\sim$ 100 mW/cm<sup>2</sup>) illumination and the system was calibrated with a National Renewable Energy Laboratory (NREL)-certified standard 2 cm  $\times$  2 cm silicon photodiode with a KG5 filter. The current-voltage curves were measured using a Keithley 2400 source meter.

*EQE measurement:* EQE spectra were measured using a PV Measurements Inc QEX7 system at a frequency of 120 Hz and lock-in time constant of 1 sec. The EQE system was calibrated with a NIST-calibrated silicon photodiode.

### *MIS-CELIV experiments:*

In the following, we briefly explain the working principles of the technique. MIS-CELIV uses a metal-insulator-semiconductor architecture where  $\text{MgF}_2$  is the insulator (dielectric) layer. To perform the experiment, as shown in Figure S6a, an initial offset voltage is applied to the device ( $t < 0$ ), which injects one type of carrier (holes or electrons depending on the polarity and the position of the insulator layer). To be able to inject charge carriers, the work function of the injecting electrode is of importance. For the hole-only devices the architecture was ITO/ $\text{MgF}_2$ /semiconductor/MoOx/Ag and for the electron-only devices ITO/ $\text{MgF}_2$ /semiconductor/Al. The offset voltage is such that the potential is positive on the MoOx/Ag electrode for the former to inject holes, and negative on Al for the later to inject electrons. At sufficiently large offset voltage ( $V_{\text{off}} \gg KT/e$ ) a thin sheet of charges is formed at the interface with the insulator. A triangle voltage pulse in the opposite direction of the offset polarity is then applied to extract the injected charges, which are accumulated at the interface. In this case the current initially reaches a displacement level ( $j^0$ ), which corresponds to the capacitance of the whole diode Figure S6b. Then the current increases until reaching a peak when the charge carriers reach the electrode (transit time). In the case of applying a large voltage offset, the amount of injected carriers is large enough so that at the start of the extraction, the current increases to a secondary displacement level with a quadratic behaviour versus time as a result of forming space charges within the semiconductor where the electric field is screened. The secondary displacement current corresponds to the capacitance level of the dielectric layer, which is chosen to be larger than the capacitance of the whole diode. The transit time of the carriers can then be measured very precisely as the time it takes until the current reaches  $2j^0$ . From the transit time it is possible to calculate the mobility of the relevant carrier.

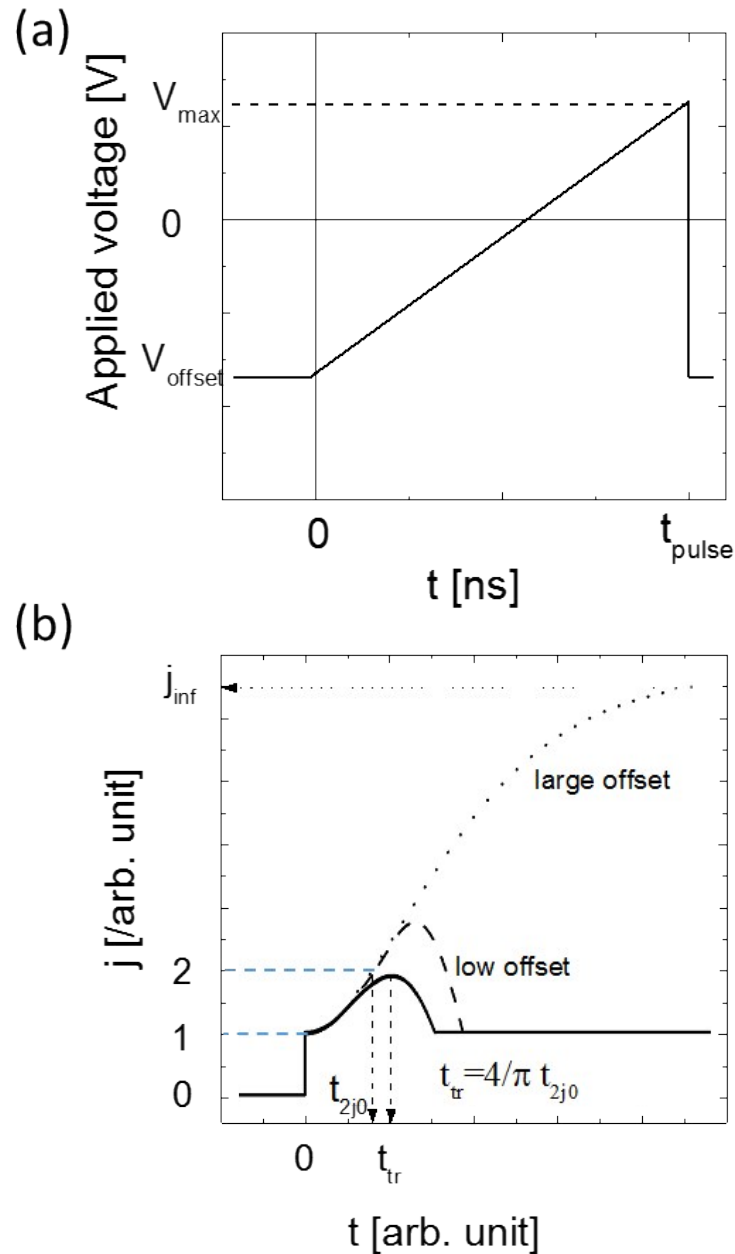


**Figure S6.** (a) Applied CELIV voltage pulse used to perform MIS-CELIV. A voltage offset is applied initially in forward bias direction to inject the carriers (holes or electrons) and the triangle voltage extracts the injected carriers, which can be accumulated near the interface of semiconductor/dielectric layer; (b) Schematic MIS-CELIV current transients for different offset voltages. In the case of a small offset the extraction peak is the charge carrier transit time. For larger offset voltages space charges form during the extraction and the carrier transit time can be calculated from  $t_{2j0}$  as shown in the figure.

Metal-Insulator-Semiconductor diode devices were prepared from ITO/PEDOT:PSS substrates (Kintec) prepared which were cleaned as detailed above for solar cell devices. A 50 nm layer of magnesium fluoride ( $\text{MgF}_2$ ) was deposited onto cleaned ITO by thermal evaporation of  $\text{MgF}_2$  pellets from a molybdenum metal boat under a vacuum of  $10^{-6}$  mbar at a rate of  $0.2 \text{ \AA/s}$ . After deposition of the active layer on the  $\text{MgF}_2$  (concentration of 20 mg/mL and spin rate of 200 rpm for neat 2 and total concentration of 20 mg/mL and spin rate of 500 rpm for 2:PC<sub>70</sub>BM),  $\text{MoO}_3$  (5 nm)/Ag (50 nm) or Al (80 nm) electrodes were deposited on the top for hole- and electron-only devices, respectively. For the MIS-CELIV measurements, an arbitrary waveform generator (Agilent 33250A) was used to generate the CELIV triangle pulse with adjustable voltage slope and offset. The signal was recorded using a digital storage oscilloscope (LeCroy Waverunner A6200). More details about the experimental setup are provided herein<sup>6</sup>.

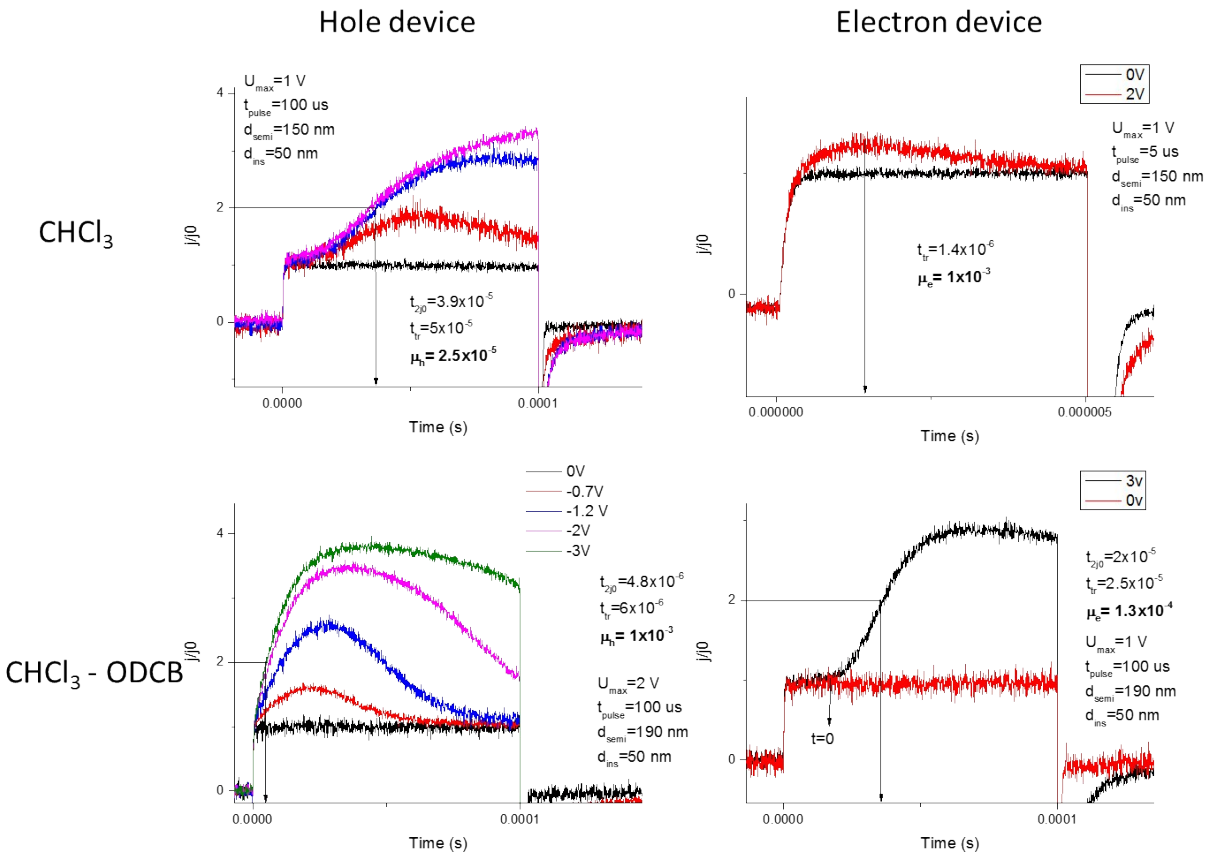


**Figure S7.** MIS-CELIV transients for 2:PC<sub>70</sub>BM blends cast from CF and CF + 7% ODCB.

## References

- 1) D. Gendron, E. Gann, K. Pattison, F. Maasoumi, C. R. McNeil, S. E. Watkins, P. L. Burn, B. J. Powell, P. E. Shaw, *J. Mater. Chem. C*, 2014, **2**, 4276-4288.
- 2) M. W. Schmidt, K. K. Baldridge, J. A. Boatz, S. T. Elbert, M. S. Gordon, J. H. Jensen, S. Koseki, N. Matsunaga, K. A. Nguyen, S. Su, T. L. Windus, M. Dupuis, J. A. Montgomery *J. Comput. Chem.* 1993, **14**, 1347-1363.
- 3) M. S. Gordon, M. W. Schmidt "Advances in electronic structure theory: GAMESS a decade later" pp. 1167-1189, in "Theory and Applications of Computational Chemistry: the first forty years" C. E. Dykstra, G. Frenking, K. S. Kim, G. E. Scuseria (editors), Elsevier, Amsterdam, 2005.
- 4) M. Ullah, T. B. Singh, H. Sitter, N. S. Sariciftci, *Appl. Phys. A: Mater. Sci. Process.*, 2009, **97**, 521-526.
- 5) G. Schwabegger, M. Ullah, M. Irimia-Vladu, M. Reisinger, Y. Kanbur, R. Ahmed, P. Stadler, S. Bauer, N.S. Sariciftci, H. Sitter. *Synth. Met.*, 2011, **161**, 2058-2062.
- 6) A. Armin, M. Velusamy, P. L. Burn, P. Meredith, A. Pivrikas, *Appl. Phys. Lett.*, 2012. **101**, 083306.